JACS
JOURNAL OF THE AMERICAN CHEMICAL SOCIETY

Article

Coupled X-Ray Absorption/ UV-Vis Monitoring of Fast Oxidation Reactions Involving a Non-Heme Iron Oxo Complex.

Giorgio Capocasa, Francesco Sessa, Francesco Tavani, Giorgio Olivo, Manuel Monte, Sakura Pascarelli, Osvaldo Lanzalunga, Stefano Di Stefano, and Paola D'Angelo

J. Am. Chem. Soc., **Just Accepted Manuscript** • Publication Date (Web): 16 Jan 2019

Just Accepted

ACS Publications

is published by the American Chemical Society. 1155 Sixteenth Street N.W., Washington, DC 20036

Coupled X-Ray Absorption/ UV-Vis Monitoring of Fast Oxidation Reactions Involving a Non-Heme Iron Oxo Complex.

Giorgio Capocasa,[†, §,¶] Francesco Sessa,[†,¶] Francesco Tavani,[†, ¶] Manuel Monte,[‡] Giorgio Olivo,[†] Sakura Pascarelli,[‡] Osvaldo Lanzalunga,[†, §,*] Stefano Di Stefano,[†,§,*] and Paola D'Angelo,[†,*]

[†] Dipartimento di Chimica, Università di Roma "La Sapienza", P.le A. Moro 5, 00185 Roma, Italy.

[‡] European Synchrotron Radiation Facility, 71, Avenue des Martyrs, Grenoble, France.

[§] Istituto CNR di Metodologie Chimiche (IMC-CNR), Sezione Meccanismi di Reazione, P.le A. Moro 5, 00185 Roma, Italy.

ABSTRACT: Time-resolved X-ray absorption (XAS) and UV-Vis spectroscopies with millisecond resolution are used simultaneously to investigate oxidation reactions of organic substrates by non-heme iron activated species. In particular, the oxidation processes of arylsulfides and benzyl alcohols by a non-heme iron oxo-complex have been studied. We show for the first time that the pseudo first-order rate constants of fast bimolecular processes in solution (milliseconds and above) can be determined by time-resolved XAS technique. By following the Fe K-edge energy shift it is possible to detect the rate of iron oxidation state evolution that matches that of the bimolecular reaction in solution. The kinetic constant values obtained by XAS are in perfect agreement with those obtained by means of the concomitant UV-Vis detection. This combined approach has the potential to provide unique insights into reaction mechanisms in the liquid phase that involve changes of the oxidation state of a metal center and it is particularly useful in complex chemical systems where possible interferences from species present in solution could make impossible the use of other detection techniques.

INTRODUCTION

The comprehension of reactivity is one of the main topics of chemical science since its very beginning. The knowledge of the reaction mechanisms is indeed an indispensable tool to control chemical transformations and to direct them into the desired outputs. Due to the increasing complexity of the chemical systems investigated by contemporary researchers, the need is strong for innovative techniques capable of providing both an easy and selective monitoring of the process of interest. This exigency is even stronger when chemical reactions are fast on human timescales (seconds and below).

X-ray absorption spectroscopy (XAS) allows one to gain information on the local structure and electronic configuration of a selected atom both on solid and liquid systems. It is therefore a very powerful tool to follow the structural and electronic evolution taking place during chemical reactions that generally occur in solution on a timescale of milliseconds and above. In a pioneering investigation time-resolved energy dispersive X-ray absorption spectroscopy (EDXAS) was synchronized with a stopped flow experiment to monitor the reactions involving nickel, iron and iridium complexes. This work showed the potentialities of this combined approach.[1] Afterward, simultaneous structural and kinetic information was obtained from a combined stopped flow, UV-Vis spectroscopy and energy dispersive extended X-ray absorption fine structure (EXAFS) experiment on a two-step prototypical oxidative reaction of Pd complexes in solution. This reaction occurs in the second time scale and this allowed EXAFS spectra to be collected.[2] Further, a combined in-situ UV-Vis XAS spectroscopic setup showed that radiation damage may occur during in situ reactions of copper containing samples.[3]

Recently, we have shown that time-resolved EDXAS and UV-Vis spectroscopy can be used in combination, to follow fast chemical processes (halftimes from milliseconds to seconds) by the direct observation of the intermediates succeeding one another during the reaction.[4] In particular, time-resolved XAS allowed us to monitor the evolution of the oxidation state of the iron metal center present in the prototypical non-heme complex Fe^{II}(tris(2-pyridylmethyl)amine) ($[TPA{\bullet}Fe^{II}]^{2+}$) and of the first coordination sphere around the metal itself, when the complex was subjected to the action of oxidizing species like hydrogen peroxide or peroxyacetic acid ($AcOO_2H$). Concomitant UV-Vis monitoring of the reaction enabled us to unambiguously assign the identities to the several reaction intermediates. Experimentally, XAS and UV-Vis techniques were coupled by means of perpendicular detections carried out in the probe of a stopped-flow apparatus.

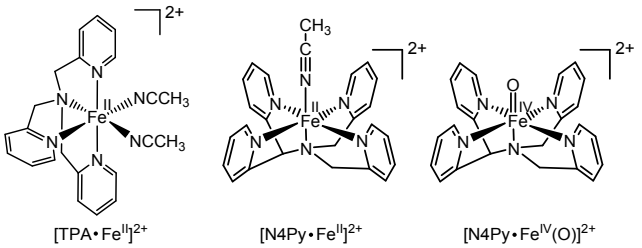

Figure 1. Molecular structures of the non-heme iron complexes.

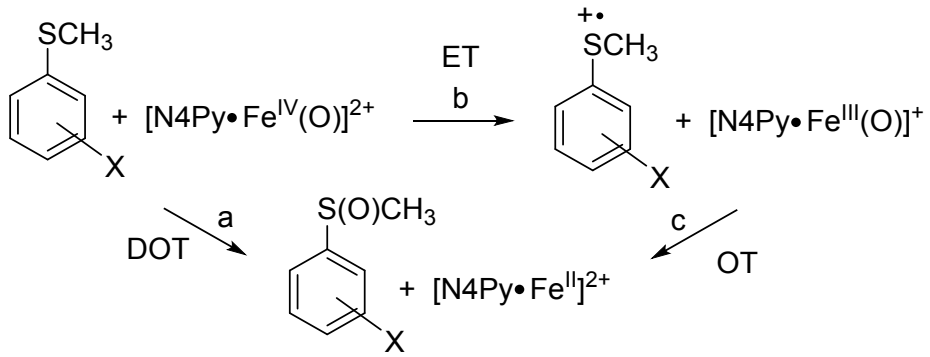

Scheme 1. Mechanistic dicothomy in the $[N_4Py{\bullet}Fe^{IV}(O)]^{2+}$ oxydation of arylsulfide: (a) the DOT mechanism, (b-c) the ET-OT mechanism.

Here, we report that the use of the time resolved XAS/UV-Vis coupled technique is not limited to the analysis of the activation of the metal complex in the presence of suitable oxidants but it can also be extended to the investigation of the oxidation reactions of organic substrates by the non-heme iron activated species. In particular, we have focused our attention on the oxidation processes of synthetic interest such as sulfide and alcohol oxidation, by the oxo-complex $[N_4Py{\bullet}Fe^{IV}(O)]^{2+}$ derived from the other paradigmatic non-heme iron complex $[N_4Py{\bullet}Fe^{II}]^{2+}$ (N_4Py=N,N-bis(2-pyridylmethyl)-N-bis(2-pyridyl)methylamine) reported in Figure 1. In this work, we show for the first time that the pseudo first-order rate constants of fast bimolecular processes in solution (milliseconds and above) can be determined by the time-resolved XAS technique. In particular, following the Fe K-edge energy shift it is possible to determine the rate of the iron oxidation state evolution that matches that of the bimolecular reaction in solution. The kinetic constant values obtained by XAS are indeed in perfect accordance with those obtained by means of the concomitant UV-Vis detection.

This innovative approach was possible using the energy dispersive XAS technique now available at third generation synchrotron light sources that allows one to collect time resolved X-ray absorption near edge spectra with good signal to noise ratio with a time resolution of 10 ms for photoabsorber concentrations of few mM under operand conditions.

The choice of $[N_4Py{\bullet}Fe^{IV}(O)]^{2+}$ as the oxidizing agent was guided by both the ever-growing interest on non-heme iron complexes as catalysts for the oxidation of organic compounds mainly due to the cheap and environmentally friendly conditions under which these kind of reactions can be carried out,[5-10] and the high stability of such particular oxo-complex that guarantees easy manipulation and monitoring.[11,12]

RESULTS AND DISCUSSION

The XAS/UV-Vis coupled technique was used to follow the oxidation of a series of thioanisoles, differently substituted in the para position of the aromatic ring, to the corresponding methylphenyl sulfoxide (CH_3CN, 25 °C) by the oxidant $[N_4Py{\bullet}Fe^{IV}(O)]^{2+}$ freshly prepared by reaction between $[N_4Py{\bullet}Fe^{II}]^{2+}$ and peroxyacetic acid. In general, sulfoxidation of aryl sulfides promoted by high-valent iron(IV)-oxo complexes in non-heme iron oxygenases and their synthetic non-heme models is characterized by a mechanistic dichotomy between the direct oxygen transfer or "oxene process" (DOT) and electron transfer followed by oxygen transfer (ET-OT) mechanisms.[13-18] As reported by Nam and Fukuzumi, sulfoxidation of thioanisoles promoted by $[N_4Py{\bullet}Fe^{IV}(O)]^{2+}$ occurs by a DOT mechanism (Scheme 1, path a) in the absence of acid additives or in the presence of perchloric acid (70% $HClO_4$).[19,20] A mechanistic switch to an ET-OT mechanism or better to a metal ion-coupled electron transfer/proton-coupled electron transfer occurs when the same reaction is carried out in the presence of $Sc(OTf)_3$ or triflic acid (HOTf), respectively (Scheme 1, path b,c).[19,21] An ET reaction followed by a fast oxygen rebound is also operating in the sulfoxidation of cumyl or arylethyl aryl sulfides promoted by $[N_4Py{\bullet}Fe^{IV}(O)]^{2+}$ and other high-valent iron-oxo complexes.[22-24] Under our conditions, where no additive other than $[N_4Py{\bullet}Fe^{IV}(O)]^{2+}$ is added, the aryl sulfides oxidation should proceed through a simple DOT mechanism (Scheme 1, path a), that is an elementary reaction. Figure 2 shows the results related to the oxidation of thioanisole ($PhSCH_3$) by $[N_4Py{\bullet}Fe^{IV}(O)]^{2+}$. The reaction was carried out under pseudo-first order conditions with the concentration of PhSMe (350 mM) exceeding that of $[N_4Py{\bullet}Fe^{IV}(O)]^{2+}$ (15 mM) by a factor of 23. Figure 2A shows the continuous evolution of the Fe K-edge normalized time-resolved EDXAS spectra during the course of the reaction.

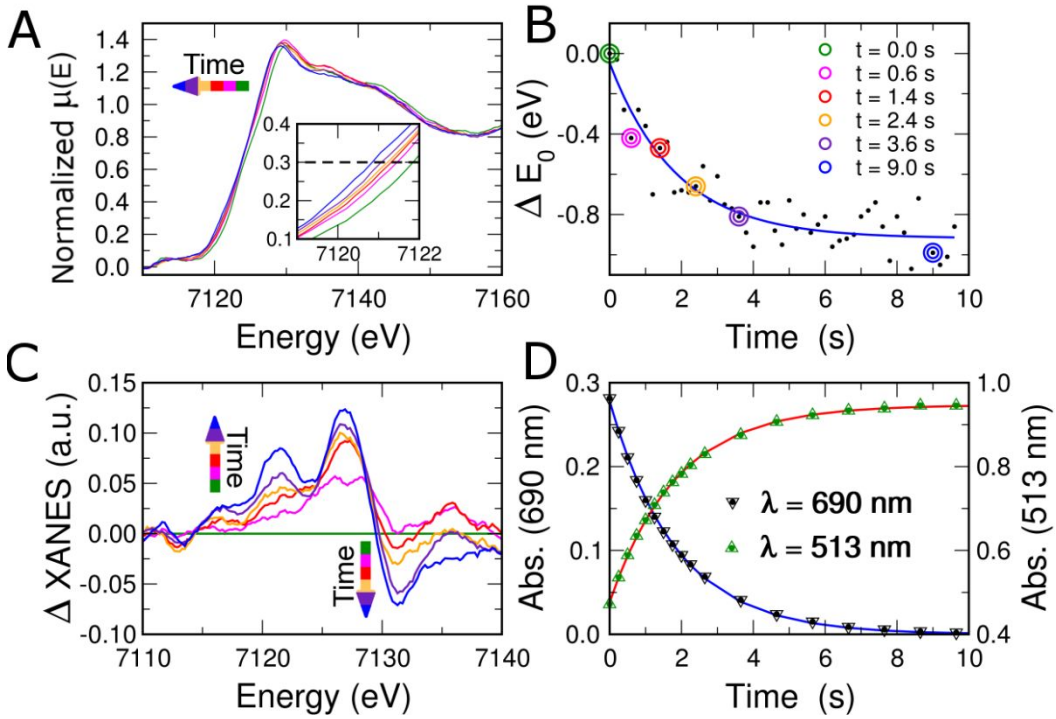

Figure 2. Oxidation of PhSMe by $[N_4Py{\bullet}Fe^{IV}(O)]^{2+}$ in CH_3CN at 25 °C followed by the coupled XAS/UV-Vis technique. (A) Time evolution of the XANES spectra at selected times from reaction start. A magnification of Fe K-edge region is shown in the inset. (B) ΔE_o vs time (the points with colored marks correspond to the spectra with the same color reported in panels A and C). ΔE_o is the difference between the K-edge energy position of the XANES spectra at time t and the K-edge position of the first XANES spectrum at t=0 s. Blue curve derives from a first-order kinetic treatment of experimental points. (C) Difference between the XANES spectrum at time t and XANES spectrum at t=0 s related to panel A. (D) UV/Vis monitoring of $[N_4Py{\bullet}Fe^{IV}(O)]^{2+}$ (downward triangles at λ=690 nm) and $[N_4Py{\bullet}Fe^{II}]^{2+}$ (upward triangles at λ=513 nm) during the reaction. Blue and red curves are derived from a first-order kinetic treatment of experimental points.

The XANES spectra show a shift of the Fe K edge position towards lower energy values due to the reduction of the iron oxidation state from Fe^{IV} to Fe^{II} during the reaction. The time resolved EDXAS spectra were recorded every 120 ms and the reaction was followed for 10 s. Previous works have demonstrated the potential of Fe K-edge XANES spectroscopy for the quantitative determination of Fe^{II}/Fe^{III} ratio in different materials.[25-28] The X-ray absorption Fe K-edge comprises features that have been ascribed to transition from core to bound states, namely 1s→3d (pre-edge), 1s→4s (edge shoulder) and 1s→4p (edge crest). The 1s→4s transition usually forbidden is enabled by strong orbital mixing between the 4s and 4p orbitals.[27,28] The energy of the 1s→4s edge shoulder was found to correlate linearly with the iron oxidation state.[27] Exploiting this potential we have followed the variation of this spectral feature to detect the rate of reduction of Fe^{IV} to Fe^{II} during the reaction. In particular, we measured the energy of the main absorption edge at a height of 0.3 as a function of time. The value 0.3 was chosen in an attempt to determine the energy of the threshold while minimizing the distortions arising from transitions to bound states. Note that this value has been chosen looking at the difference spectra shown in Figure 2C and it corresponds to the first maximum region of the difference spectra. Figure 2B shows the evolution of ΔE_0 during the reaction, where ΔE_0 is the difference between the Fe K-edge energy position of the XANES spectra at time t and the edge position of the first XANES spectrum at t=0 s. The blue curve in Figure 2B is the first-order kinetic plot obtained by fitting the experimental data with the following equation:

$$\Delta E_0(t) = [E_0(i) - E_0(f)]e^{-kt} + E_0(f) \qquad (1)$$

where $E_o(i)$ is the K-edge energy at t=0 s, $E_o(f)$ is the K edge energy at the end of the reaction and k is the kinetic constant. From this analysis the k value turned out to be 0.54±0.06 s^{-1}.

Spectrophotometric data related to the experiment are reported in Figure 2D. Absorbance variation at 513 nm is due to the increase of the concentration of $[N_4Py{\bullet}Fe^{II}]^{2+}$ which is the reduction product of $[N_4Py{\bullet}Fe^{IV}(O)]^{2+}$. The concentration decrease of the latter species is confirmed by the concomitant decrease of the absorbance at 690 nm, the maximum visible absorption wavelength of

this species and by the shift of the XANES Fe K-edge. Red and blue curves in Figure 2D are first-order kinetic plots with independently obtained kinetic constants of k of 0.53±0.02 and 0.54±0.02 s^{-1}, respectively, well in keeping with literature data.[29,30] It was gratifying to observe that

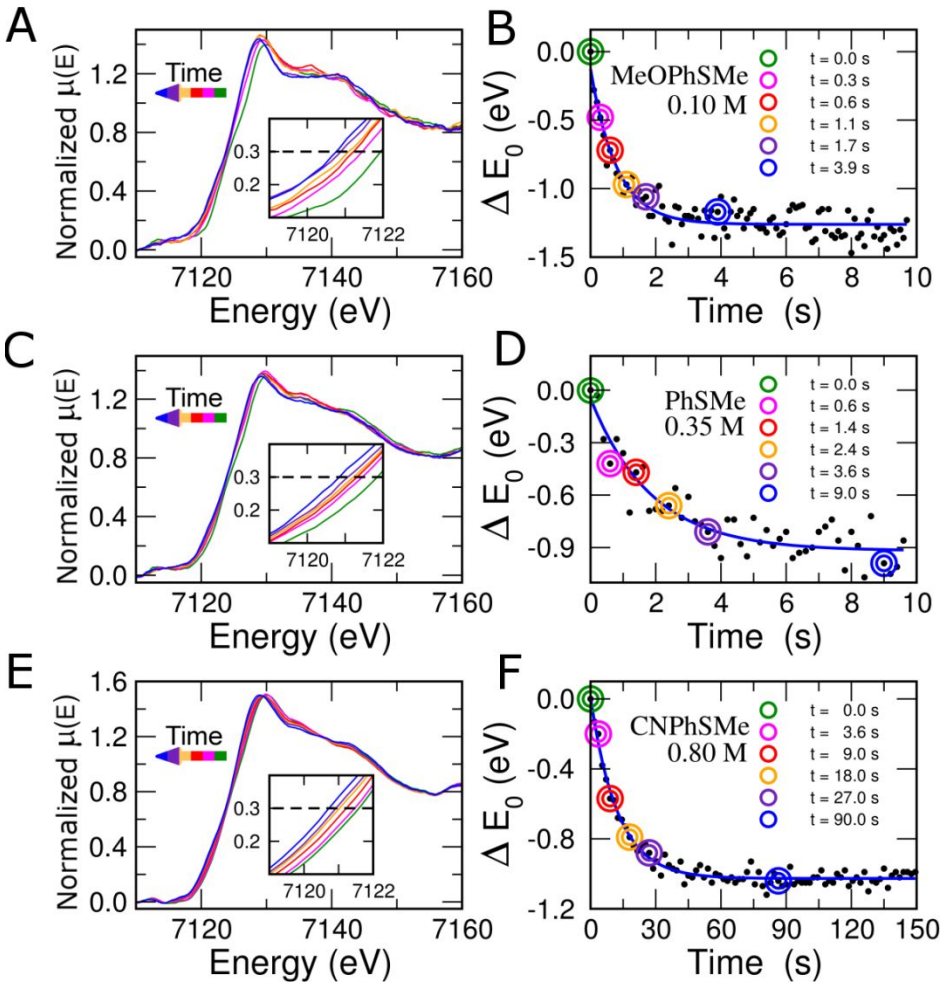

Figure 3. Time evolution of the Fe K-edge EDXAS spectra of the reactions between (A) p-$CH_3OC_6H_4SCH_3$ (MeOPhSMe), (C) $PhSCH_3$ and (E) p-$CNC_6H_4SCH_3$ (CNPhSMe) with $[N_4Py{\bullet}Fe^{IV}(O)]^{2+}$ in CH3CN at 25 °C. Magnifications of Fe K-edge regions are shown in the insets. (B,D,F) ΔE_o vs time (the points with colored marks correspond to the spectra with the same color reported in panels A,C,E). ΔE_o is the difference between the edge energy position of the XANES spectra at time t and the edge position of the first XANES spectrum at t=0 s. Blue curves in panel B, D, F derive from a first-order kinetic treatment of EDXAS experimental points.

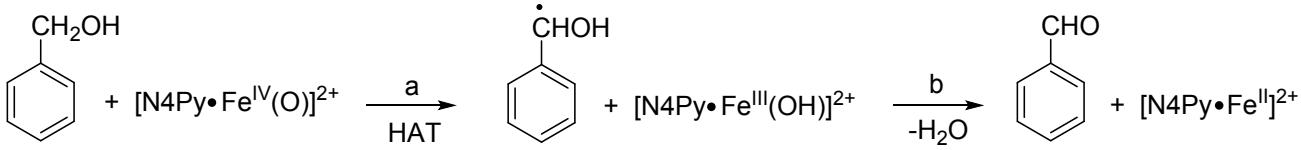

Scheme 2. Mechanism for the oxidation of benzyl alcohol by $[N_4Py{\bullet}Fe^{IV}(O)]^{2+}$. After a rate determining hydrogen atom transfer from the benzylic C-H bond to the oxidant a fast second oxidation and a subsequent proton loss from intermediate lead to benzaldehyde.

these values are identical to that obtained from the EDXAS spectra. This experiment proofs that the quantitative analysis of the shift of the XANES E_o value during the reaction, which is a direct observation of the change of the iron metal oxidation state from Fe^{IV} to Fe^{II}, may serve for the kinetic analysis of fast reacting chemical systems (in this case a half-life of 1.3 s is measured).

In order to investigate the potentiality of time-resolved XAS technique for kinetic measurements we also used other arylsulfides with different reactivity, whose oxidation by $[N_4Py{\bullet}Fe^{IV}(O)]^{2+}$ is known to be faster and slower than that of PhSMe. Thus, *para*-methoxy and *para*-cyano thioanisoles were also included in this study and the related results are shown in Figure 3 where selected XANES

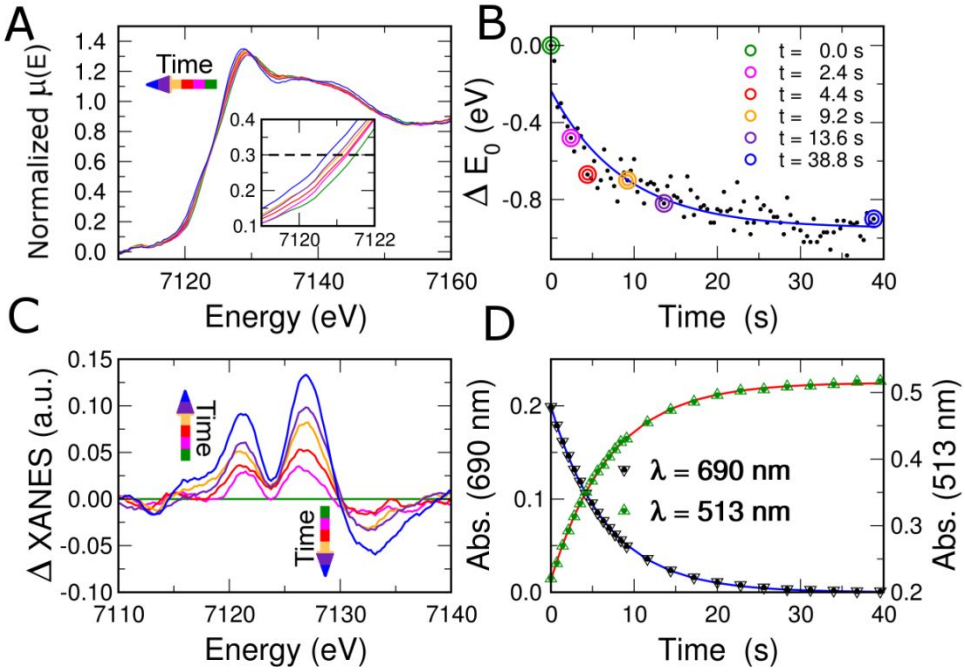

Figure 4. Oxidation of $PhCH_2OH$ by $[N_4Py{\bullet}Fe^{IV}(O)]^{2+}$ in CH_3CN at 25 °C followed by the coupled XAS/UV-Vis technique. (A) Time evolution of the XANES spectra at selected times from reaction start. A magnification of Fe K-edge region is shown in the inset. (B) ΔE_o vs time (the points with colored marks correspond to the spectra with the same color reported in panel A). ΔE_o is the difference between the K-edge energy position of the XANES spectra at time t and the K-edge position of the first XANES spectrum at t=0 s. Blue curve derives from a first-order kinetic treatment of experimental points. (C) Difference between the XANES spectrum at time t and XANES spectrum at t=0 s related to panel A. (D) UV-Vis monitoring of $[N_4Py{\bullet}Fe^{IV}(O)]^{2+}$ (downward triangles at λ=690 nm) and $[N_4Py{\bullet}Fe^{II}]^{2+}$ (upward triangles at λ=513 nm) during the reaction. Blue and red curves are derived from a first-order kinetic treatment of experimental points.

spectra at different times and ΔE_0 experimental data points with the related first-order fits carried out with eq. (1) are reported. The reactions were carried out under pseudo first-order kinetic conditions, p-$CH_3OC_6H_4SCH_3$ 100 mM + $[N4Py{\bullet}Fe^{IV}(O)]^{2+}$ 15 mM and p-$CNC_6H_4SCH_3$ 800 mM + $[N_4Py{\bullet}Fe^{IV}(O)]^{2+}$ 15 mM in CH_3CN at 25 °C. As expected the para-methoxy derivative is significantly more reactive than the parent compound and the reaction was followed for 10 s while collecting the EDXAS spectra every 100 ms (Figure 3A). The first order kinetic constant obtained by fitting the ΔE_0 values as a function of t with eq (1) (Figure 3B) was k of 1.23±0.05 s^{-1} (half-life 0.56 s). Conversely, the para-cyano derivative is less reactive in this case the EDXAS spectra were collected

every 1.8 s and the reaction was followed for 150 s (Figure 3E). The first order kinetic constant as determined from the XANES spectra (Figure 3F) was k = 0.08±0.04 s^{-1} (half-life 8.6 s). These values, the latter of which is in good accordance with literature data,[31] reflect the electrophilic character of the oxidizing species $[N_4Py{\bullet}Fe^{IV}(O)]^{2+}$.

In order to further check the reliability of our results a different method based on the deconvolution of the threshold region of the Fe K-edge spectra as a sum of an arctangent function describing the transition into the continuum, and a Lorentzian function representing the 1s→4s transition has been carried out. This analysis has been applied to the oxidation of p-$CH_3OC_6H_4SCH_3$ by $[N_4Py{\bullet}Fe^{IV}(O)]^{2+}$ providing the same value of the kinetic constant within the experimental error (see SI for details).

The XAS/UV-Vis coupled technique was also used to follow the oxidation of benzyl alcohol to benzaldehyde by $[N_4Py{\bullet}Fe^{IV}(O)]^{2+}$. This reaction has a more complex mechanism than that related to the $[N_4Py{\bullet}Fe^{IV}(O)]^{2+}$ oxidation of the aryl methylsulfides, which is reported in Scheme 2. The mechanistic details of the oxidation of benzyl alcohol with $[(N_4Py)Fe^{IV}(O)]^{2+}$ have been disclosed by Nam and coworkers.[32] From the results of the oxidation of benzyl alcohol with an ^{18}O labeled iron(IV)-oxo complex, $[N_4Py{\bullet}Fe^{IV}(^{18}O)]^{2+}$, it was found that the oxygen atom in the benzaldehyde product does not derive from the ferryl oxygen atom. Thus benzaldehyde is formed by a first hydrogen atom transfer (HAT) from the benzylic C-H bond to $[N_4Py{\bullet}Fe^{IV}(O)]^{2+}$ to produce the α-hydroxybenzyl radical and the iron hydroxo complex $[N_4Py{\bullet}Fe^{III}(OH)]^{2+}$ (step a in Scheme 2). In the second step, a second fast oxidation of the former species followed by proton loss leads to products, as reported in path b of Scheme 2. Figure 4 shows the results obtained when the XAS/UV-Vis coupled technique was applied for monitoring the reaction of Scheme 2. Again, the reaction was carried out under pseudo-first order conditions (benzyl alcohol 2.18 M and $[N_4Py{\bullet}Fe^{IV}(O)]^{2+}$ 15 mM). The panels of the Figure 4 have to be read with the same rational of those of Figure 2. UV-Vis experimental data points (Figure 4D) related to the disappearance of $[N_4Py{\bullet}Fe^{IV}(O)]^{2+}$ followed at λ= 690 nm and appearance of $[N_4Py{\bullet}Fe^{II}]^{2+}$ (absorption at λ = 513 nm), fitted with a first order equation gave *k* values of 0.15±0.01 s^{-1} and 0.14±0.01 s^{-1} (half-life 4.7 s), respectively, which are again in accordance with literature data.[33] In this case the EDXAS spectra were recorded every 300 ms and the reaction was followed for 40 s (Figure 4A). The first order treatment of the related XANES ΔE_o values vs t data reported in Figure 4B provided a *k* value of 0.11±0.05 s^{-1} (half-life 6.2 s) which, within the experimental error, coincides with the values obtained from UV-Vis data, again confirming the validity of the time-resolved XAS technique in the kinetic analysis of fast chemical reactions.

CONCLUSION

In this work we show that it is possible to use the time resolved XAS technique to carry out kinetic measurements related to bimolecular fast chemical reactions in solution. In particular, it is demonstrated that, when the EDXAS and UV-Vis techniques are coupled by means of perpendicular detections in the probe of a stopped-flow apparatus, the kinetic measures derived from both XANES E_o and UV-Vis monitoring are coincident within experimental errors. This makes time resolved XAS technique a helpful tool to follow fast chemical reactions which involve changes of the oxidation state of a metal center. The advantage is particularly remarkable in complex chemical systems under reaction, where possible interferences from the species present in solution could make impossible the use of any other detection technique. Finally, a significant progress has recently been achieved concerning the development of advanced multivariate analysis able to capture the XANES signature of each species formed in the reaction course.[34-36] This approach would allow one not only to determine the kinetic constant values but also to provide a structural characterization of all the species involved in the reaction. Additional investigations are underway to pursue this goal.

ASSOCIATED CONTENT

Supporting Information. The Supporting Information is available free of charge on the ACS Publications website at DOI:

Experimental details and EDXAS data treatment.

AUTHOR INFORMATION

Corresponding Author

* p.dangelo@uniroma1.it
* stefano.distefano@uniroma1.it
*osvaldo.lanzalunga@uniroma1.it

ORCID

Giorgio Capocasa: 0000-0002-9725-2727
Paola D'Angelo: 0000-0001-5015-8410
Stefano Di Stefano 0000-0002-6742-0988
Osvaldo Lanzalunga 0000-0002-0532-1888

Author Contributions

¶Equal contribution.

Note

The authors declare no competing financial interest.

ACKNOWLEDGMENT

This work was supported by the University of Rome "La Sapienza" (Progetti Ateneo 2015 C26H159F5B). ESRF is acknowledged for the provision of synchrotron beam time.

REFERENCES

(1) Abdul Rahman, M. B. B.; Bolton, P. R.; Evans, J.; Dent, A. J.; Harvey, I.; Diaz-Moreno, S. Application of stopped flow techniques and energy dispersive EXAFS for investigation of the reactions of transition metal complexes in solution: Activation of

nickel β-diketonates to form homogeneous catalysts, electron transfer reactions involving iron(III) and oxidative addition to iridium(I). *Farday Discuss.* **2002**, *122*, 211.

(2) Guilera, G.; Newton, M. A.; Polli, C.; Pascarelli, S.; Guino, M.; Hii, K. K. In situ investigation of the oxidative addition in homogeneous Pd catalysts by synchronised time resolved UV-Vis/EXAFS. *Chem. Commun.* **2006**, *41*, 4306.

(3) Mesu, J. G.; van der Eerden, A. M. J.; de Groot, F. M. F.; Weckhuysen, B. M. Synchrotron Radiation Effects on Catalytic Systems As Probed with a Combined In-Situ UV–Vis/XAFS Spectroscopic Setup *J. Phys. Chem. B* **2005**, *109*, 4042.

(4) Olivo, G.; Barbieri, A.; Dantignana, V.; Sessa, F.; Migliorati, V.; Monte, M.; Pascarelli, S.; Narayanan, T.; Lanzalunga, O.; Di Stefano, S.; D'Angelo, P. Following a Chemical Reaction on the Millisecond Time Scale by Simultaneous X-ray and UV/Vis Spectro-scopy. *J. Phys. Chem. Lett.* **2017**, *8*, 2958.

(5) Chen, K; Que, L., Jr. Stereospecific Alkane Hydroxylation by Non-Heme Iron Catalysts: Mechanistic Evidence for an Fe^{V}═O Active Species. *J. Am. Chem. Soc.* **2001**, *123*, 6327.

(6) Chen, K.; Costas, M.; Kim, J.; Tipton, A. K.; Que, L., Jr. Olefin cis-dihydroxylation versus epoxidation by non-heme iron catalysts: two faces of an Fe(III)-OOH coin. *J. Am. Chem. Soc.* **2002**, *124*, 3026.

(7) Nam, W. High-Valent Iron(IV)–Oxo Complexes of Heme and Non-Heme Ligands in Oxygenation Reactions. *Acc. Chem. Res.* **2007**, *40*, 522.

(8) Talsi, E. P.; Bryliakov, K. P. Chemo- and stereoselective C-dihydroxylations with H. *Coord. Chem. Rev.* **2012**, *256*, 1418.

(9) Nam, W.; Lee, Y.-M.; Fukuzumi, S. Tuning reactivity and mechanism in oxidation reactions by mononuclear non heme iron(IV)-oxocomplexes. *Acc. Chem. Res.* **2014**, *47*, 1146.

(10) Oloo, W. N.; Que, L., Jr. Bioinspired Non heme Iron Catalysts for C–H and C═C Bond Oxidation: Insights into the Nature of the Metal-Based Oxidants. *Acc. Chem. Res.* **2015**, *48*, 2612.

(11) Kaizer, J.; Klinker, E. J.; Oh, N. Y.; Rohde, J.-U.; Song, W. J.; Stubna, A.; Kim, J.; Münck, E.; Nam, W.; Que, L., Jr. Non hemeFe^{IV}O complexes that can oxidize the C-H bonds of cyclohexane at room temperature. *J. Am. Chem. Soc.* **2004**, *126*, 472.

(12) Lubben, M.; Meetsma, A.; Wilkinson, E. C.; Feringa, B.; Que, L., Jr. Non heme Iron Centers in Oxygen Activation: Characterization of an Iron(III) Hydroperoxide Intermediate. *Angew. Chem., Int. Ed. Engl.* **1995**, *34*, 1512.

(13) Peñéñory, A. B.; Argüello, J. E.; Puiatti, M. Novel Model Sulfur Compounds as Mechanistic Probes for Enzymatic and Biomimetic Oxidations. *Eur. J. Org. Chem.* **2005**, *114*, 122.

(14) Baciocchi, E.; Gerini, M. F.; Lanzalunga, O.; Lapi, A.; Lo Piparo, M. G. Mechanism of the oxidation of aromatic sulfides catalysed by a water soluble iron porphyrin. *Org. Biomol. Chem.* **2003**, *1*, 422.

(15) Baciocchi, E.; Lanzalunga, O.; Malandrucco, S.; Ioele, M.; Steenken, S. Oxidation of Sulfides by Peroxidases. Involvement of Radical Cations and the Rate of the Oxygen Rebound Step. *J. Am. Chem. Soc.* **1996**, *118*, 8973.

(16) Goto, Y.; Matsui, T.; Ozaki, S.; Watanabe, Y.; Fukuzumi, S. Mechanisms of Sulfoxidation Catalyzed by High-Valent Intermediates of Heme Enzymes: Electron-Transfer vs O-xygen-Transfer Mechanism. *J. Am. Chem. Soc.* **1999**, *121*, 9497.

(17) Khenkin, A. M.; Leitus, G.; Neumann, R. Electron Transfer–Oxygen Transfer Oxygenation of Sulfides Catalyzed by the $H_5PV_2Mo_{10}O_{40}$ Polyoxometalate. *J. Am. Chem. Soc.* **2010**, *132*, 11446.

(18) Kumar, A.; Goldberg, I.; Botoshansky, M.; Buchman, Y.; Gross, Z. Oxygen Atom Transfer Reactions from Isolated (Oxo) manganese(V) Corroles to Sulfides. *J. Am. Chem. Soc.* **2010**, *132*, 15233.

(19) Park, J.; Morimoto, Y.; Lee, Y.-M.; Nam, W.; Fukuzumi, S. Metal Ion-Coupled Electron Transfer of a Nonheme Oxoiron(IV) Complex: Remarkable Enhancement of Electron-Transfer Rates by Sc^{3+}. *J. Am. Chem. Soc.* **2011**, *133*, 5236.

(20) Park, J.; Morimoto, Y.; Lee, Y.-M.; Nam, W.; Fukuzumi, S. Proton-Promoted Oxygen Atom Transfer vs Proton-Coupled Electron Transfer of a Non-Heme Iron(IV)-Oxo Complex. *J. Am. Chem. Soc.* **2012**, *134*, 3903.

(21) Park, J.; Morimoto, Y.; Lee, Y.-M.; Nam, W.; Fukuzumi, S. Unified view of oxidative C-H bond cleavage and sulfoxidation by a non heme iron(IV)-oxo complex via Lewis acid-promoted electron transfer. *Inorg. Chem.* **2014**, 53, 3618.

(22) Barbieri, A.; Di Stefano, S.; Lanzalunga, O.; Lapi, A.; Mazzonna, M.; Olivo, G. Role of electron transfer processes in the oxidation of arylsulfides catalyzed by non heme iron complexes. *Phosphorus, Sulfur and Silicon* **2017**, *192*, 241.

(23) Barbieri, A.; Del Giacco, T.; Di Stefano, S.; Lanzalunga, O.; Lapi, A.; Mazzonna, M.; Olivo, G. Electron Transfer Mechanism in the Oxidation of Aryl 1-Methyl-1-phenylethyl Sulfids Promoted by Non heme Iron(IV)–Oxo Complexes: The Rate of the Oxygen Rebound Process. *J. Org. Chem.* **2016**, *81*, 12382.

(24) Barbieri, A.; De Carlo Chimienti, R.; Del Giacco, T.; Di Ste-fano, S.; Lanzalunga, O.; Lapi, A.; Mazzonna, M.; Olivo, G.; Sa-lamone, M. Oxidation of Aryl Diphenylmethyl Sulfides Promoted by a Nonheme Iron(IV)-OxoComplex: Evidence for an Electron Transfer-Oxygen Transfer Mechanism. *J. Org. Chem.* **2016**, *81*, 2513.

(25) Westre, T.-E.; Kennepohl, P.; DeWitt, J.-G.;Hedman, B.;Hodgson, K.-O.; Solomon, E.-I. A Multiplet Analysis of Fe K-Edge 1s→3d Pre-Edge Features of Iron Complexes. *J. Am. Chem. Soc.* **1997**, *119*, 6297.

(26) D'Angelo, P.; Lucarelli, D.; Della Longa, S.; Benfatto, M.; Hazemann, J.-L.; Feis, A.; Smulevich, G.; Ilari, A.; Bonamore, A.; Boffi, A. Unusual heme iron-lipid acyl chain coordination in Escherichia coli flavohemoglobin. *Biophys. J.* **2004**, *86*, 3882.

(27) Berry, A.-J.; Yaxley, G.-M.; Woodland, A.-B.; Foran, J.-G.A XANES calibration for determining the oxidation state of iron in mantle garnet. *Chem. Geol.* **2010**, *278*, 31.

(28) Shulman, R.G.; Yafet, Y.; Eisenberger, P.; Blumberg, W.E. Observation and interpretation of X-ray absorption edges of iron compounds and proteins. *PNAS* **1976,** *73*, 1384.

(29) For thioanisole a k_2 of 0.87 M^{-1} s^{-1} is reported in ref. 20 which, under our conditions corresponds to $k=k_2\times$[Substrate] = 0.30 s^{-1} to be compared with 0.53 s^{-1}. It has to be remarked that the k value reported in ref. 20 was obtained at much lower concentrations.

(30) The fair agreement between our and literature data allows us to rule out any damage due to the X-ray beam that was previously found to occur for reactions involving copper containing samples (ref. 3).

(31) For *para*-cyano thioanisole a k_2 of 0.044 M^{-1} s^{-1} is reported in ref. 20 which, under our conditions corresponds to $k=k_2\times$[Substrate] = 0.04 s^{-1} to be compared with 0.08 s^{-1}. It has to be remarked that the k value reported in ref. 20 was obtained at much lower substrate concentrations.

(32) Oh, N. Y.; Suh, Y.; Park, M. J.; Seo, M. S.; Kim, J.; Nam, W. Mechanistic insight into alcohol oxidation by high-valent iron-oxo complexes of heme and non heme ligands *Angew. Chem. Int. Ed.* **2005**, *44*, 4235.

(33) For benzyl alcohol a k_2 of 0.10 M^{-1} s^{-1} can be calculated from data in ref. **32** which, under our conditions corresponds to $k=k_2\times$[Substrate] = 0.28 s^{-1} to be compared with 0.13 s^{-1}. It has to be remarked that the k value in reported in ref 10 was obtained in lower concentrations.

(34) Smolentsev1, G,; Guilera, G.; Tromp, M.; Pascarelli, S.; Soldato, A. V. Local structure of reaction intermediates probed by time-resolved x-ray absorption near edge structure spectroscopy. *J. Chem. Phys.* **2009**, *130*, 174508.

(35) Martini, A. ; Borfecchia, E.; Lomachenko, K. A.; Pankin, I. A. ; Negri, C. ; Berlier, G.; Beato, P.; Falsig, H.; Bordiga, S.; Lamberti, C. Composition-driven Cu-speciation and reducibility in Cu-CHA zeolite catalysts: a multivariate XAS/FTIR approach to complexity. *Chem. Sci.* **2017**, *8*, 6836.

(36) Pappas, D. K.; Martini, A.; Dyballa, M.; Kvande, K.; Teketel, S.; Lomachenko, K. A.; Baran, R.; Glatzel, P.; Arstad, B.; Berlier, G.; Lamberti, C.; Bordiga, S.; Olsbye, U.; Svelle, S.; Beato, P.; Borfecchia, E. The Nuclearity of the Active Site for Methane to Methanol Conversion in Cu-Mordenite: A Quantitative Assessment. *J. Am. Chem. Soc.* **2018**, *140*, 15270.

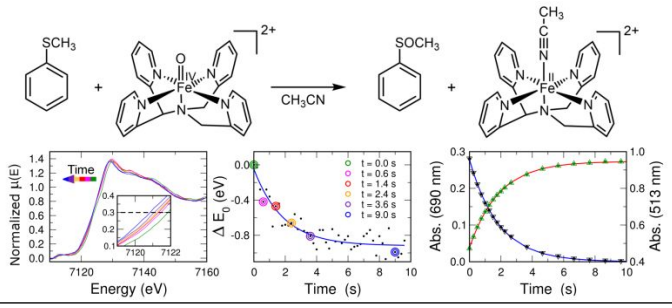
SCH3
SOCH3
CH3CN
CH3
2+
Time
Normalized μ(E)
Energy (eV)
Δ E0 (eV)
Time (s)
t = 0.0 s
t = 0.6 s
t = 1.4 s
t = 2.4 s
t = 3.6 s
t = 9.0 s
Abs. (690 nm)
Abs. (513 nm)